

Polymer-free, low tension graphene mechanical resonators

Benjamín Alemán^{*,***,1,2,3}, Michael Rousseas^{***,1,3}, Yisheng Yang¹, Will Regan^{1,2,3}, Michael Crommie^{1,2,3}, Feng Wang^{1,2,3}, and Alex Zettl^{*,1,2,3}

¹ Department of Physics, University of California at Berkeley, Berkeley, CA, 94720, USA

² Center of Integrated Nanomechanical Systems, University of California at Berkeley, Berkeley, CA, 94720, USA

³ Material Sciences Department, Lawrence Berkeley National Laboratory, Berkeley, CA, 94720, USA

Received 13 August 2013, accepted 1 October 2013

Published online ■■■

Keywords graphene, NEMS, resonators, bending rigidity, polymer-free

* Corresponding author: e-mail azettl@berkeley.edu, Phone: 1 (510) 642-4939, Fax: 1 (510) 643-8793

** Present address: Department of Physics, University of Oregon, Eugene, OR, 97403, USA

*** These authors contributed equally to this work

Graphene resonators are fabricated using a polymer-free, direct transfer method onto metal reinforced holey carbon grids. The resonators are distinguished by the absence of organic residues and excellent crystallinity. The normal mode frequencies are measured using a Fabry–Perot technique; resonance curves indicate highly linear behaviour but very little

built-in strain, which is consistent with device geometry examined by atomic force microscopy. We conclude that the oscillators' restoring force is due instead to graphene's intrinsic bending rigidity; our measurements indicate a value of approximately 1.0 eV, consistent with previous theoretical and experimental work.

© 2013 WILEY-VCH Verlag GmbH & Co. KGaA, Weinheim

1 Introduction While only one atom thick, graphene sheets are remarkably strong and stiff, allowing for the fabrication of suspended membranes with diameters on the order of microns [1–4]. Previous studies have examined the mechanical properties of graphene resonators fabricated by a variety of methods, including micro-mechanical exfoliation, under-etching of silicon substrates, and transfer of chemical vapour deposition (CVD) grown graphene to pre-defined apertures of various shapes and sizes. In almost all of these cases, the graphene comes into contact with a polymer, either from the adhesive tape used in the exfoliation process or from a layer of PMMA or similar compound used to facilitate transfer from a metal growth substrate or other surface. This introduces a significant amount of contamination to the surface of the graphene which can be very difficult to remove. These polymer residues introduce asymmetric mass loading and non-uniform strain to the graphene resonators, thereby potentially affecting their mechanical properties in ways that are difficult to predict. Additionally, these fabrication techniques tend to impart large built-in strains to the graphene resonators on the order of 0.001%, corresponding to an in-plane stress of about 1 mN/m [2].

To avoid these problems with polymer contamination and explore the possibility of controlling the tension in our

devices, we have developed a novel method for the fabrication of graphene membranes. Our suspended graphene membranes are fabricated by modifying a method previously described by the authors [5, 6]. Graphene is first grown via CVD on copper foil substrates. Next, about 100 nm of gold are evaporated onto the back side of a transmission electron microscope (TEM) grid coated with holey carbon; the gold serves to both reinforce the fragile holey carbon, as well as provide additional mass to the supports of the resonators. A small amount of isopropanol is then dropped onto the surface of the graphene-coated copper foil and the TEM grid is placed face down on top; as the isopropanol dries, the graphene adheres to the holey carbon *via* van der Waals forces. The grid and foil are then baked at 120 °C for 20 minutes to assist in evaporating excess isopropanol and to strengthen the bond of the graphene to the holey carbon. Subsequently, the copper is etched by floating the film on the surface of an etchant solution with the grid on top. In subsequent cleaning steps, the grid is floated face down on the surface of deionized water and only the flat, continuous surface of the graphene comes into contact with water. When the grid is removed and the water evaporates, it cannot pull the membrane down along the walls of its supports; as a consequence,

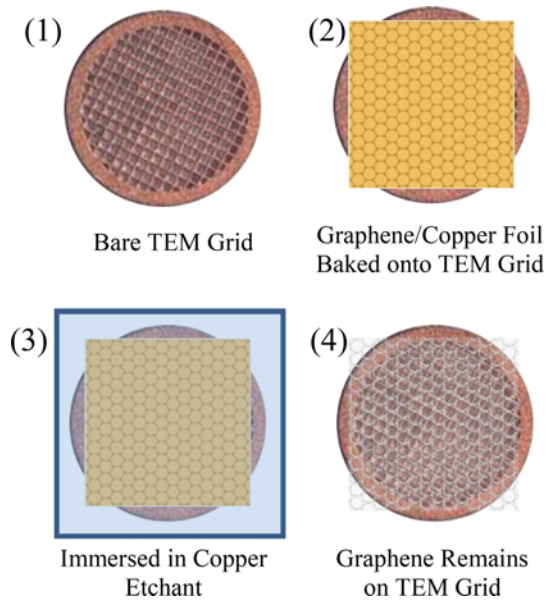


Figure 1 Polymer-free transfer process for suspended graphene resonators. The TEM grids are 3 mm in diameter.

little or no surface tension is imparted to the membrane as the water dries.

Figure 2a shows an atomic force microscope (AFM) image of a graphene sheet suspended over a 2.0 μm holey carbon support. The height profile along the dashed line is shown in Fig. 2c. The membrane is slightly buckled downwards, indicating that it is indeed tension-free. The step edges at either end of the membrane are due to a lip which is present on the rim of the holes in the carbon film.

Figure 2b shows a TEM image of an identical graphene resonator. There are no visible traces of residue on the surface of the resonator. At higher magnification (Fig. 2d), small amounts of amorphous carbon can be seen, likely left

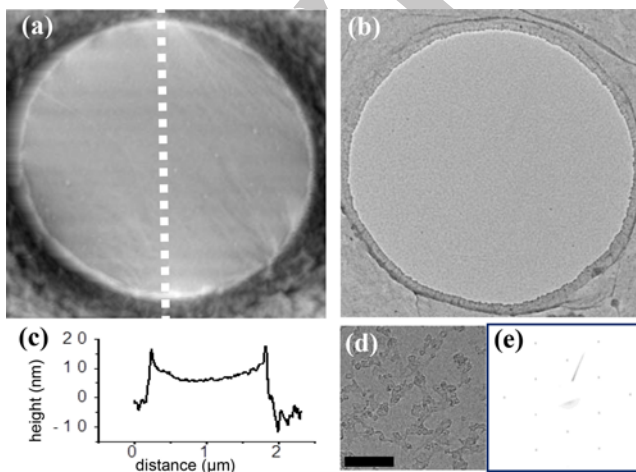


Figure 2 (a) AFM and (b) TEM images of a 2 μm diameter graphene resonator; (c) the height profile along the dashed line in image (a); (d) high magnification TEM image of membrane in (c), scale bar 10 nm; (e) electron diffraction from image (c).

by the isopropanol or the etchant solution. Figure 2e shows an electron diffraction pattern taken over the entire membrane. The presence of a single hexagonal pattern whose intensity changes monotonically with tilt angle indicates that they are comprised of a single grain of highly crystalline monolayer graphene [7].

We measure the normal mode frequencies of the membranes using an optical transduction technique, similar to that employed by other groups [2, 8]. The TEM grid onto which the graphene membranes have been mounted are taped to polished silicon wafers, such that a gap of a few microns is formed between the suspended graphene and the polished face of the wafer. This results in a Fabry–Perot device where the vibrating membrane forms one of the walls. The device is mounted into a vacuum chamber which is evacuated to approximately 1 μTorr . A 532 nm diode laser with an output power of 100 μW is directed at the graphene membrane after being focused down to a spot size of about 2 μm by an objective lens located just outside the vacuum chamber. The intensity of light reflected from the device is measured with a fast photodiode.

The resonator is driven by a separate 420 nm diode laser with a variable output between 1 mW and 5 mW and which is filtered out prior to reaching the photodiode. The laser intensity is modulated by about 100 μW using a frequency generator which is swept across the relevant range of normal mode frequencies for the membranes, between 300 kHz and 2 MHz. This fluctuation of laser power in turn modulates the temperature of the graphene and drives the resonator parametrically. The driving signal is used as a reference for a lock-in amplifier, which in turn is fed the signal from the photodiode. It should be noted that owing to the influx of power from the lasers, the temperature of the resonators is estimated to be about 500–700 $^{\circ}\text{C}$.

Figure 3 shows the amplitude and phase responses of the fundamental mode of a 2.0 μm diameter circular membrane. The amplitude response closely follows a Lorentzian shape expected from a harmonic oscillator with linear damping. The resonance frequency is 724.4 kHz with a quality factor of about 700. Typical values for a series of

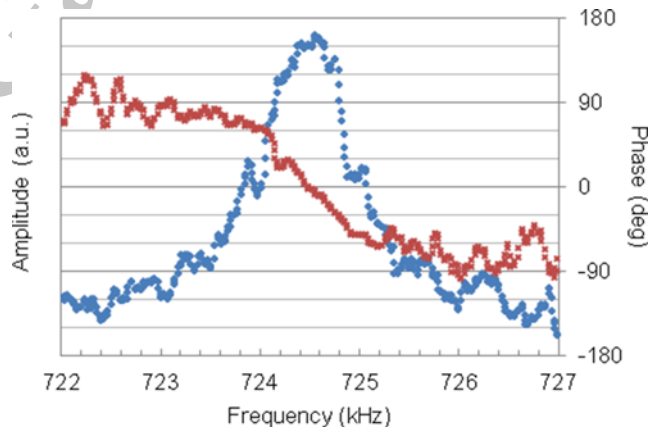


Figure 3 The amplitude (blue) and phase (red) response of a 2 μm diameter graphene membrane.

such resonators ranged from 650 kHz to 780 kHz with quality factors in the range 600 to 950. The 180° shift in the relative phase of the resonators further indicates a linear response. The equation of motion for a thin, isotropic elastic surface is given in the Kirchoff–Love theory of plates by

$$(\kappa \nabla^4 - S \nabla^2) w = q(x_1, x_2, t) - \sigma \dot{w} - \beta \ddot{w}, \quad (1)$$

where w is the out-of-plane displacement of the membrane, κ is the bending rigidity, S is the built-in surface stress, q is the time-dependent load or driving force, σ is the areal density, and β is a linear damping coefficient [9]. For most graphene resonators studied in the literature, the surface stress term dominates, and the bending rigidity can be ignored. In this model, the eigenfrequencies are proportional to $\sqrt{S/\sigma A}$, where A is the area of the resonator. For our devices, this would imply a surface stress of about 2.5 $\mu\text{N/m}$; assuming an elastic modulus of 1 TPa, this corresponding to a built-in strain of only 10^{-9} . Assuming an amplitude of 0.1 nm, this small number is of the same order of magnitude as the strain due to the oscillations themselves, implying an amplitude-dependent response, in conflict with the highly linear behaviour observed in the amplitude and phase responses of the resonators.

On the other hand, we may consider the case where the bending rigidity dominates. In this model the fundamental harmonic for a circular plate which is clamped at its circumference is given by $f = 5.108 \sqrt{\kappa/\sigma A^2}$ [9]. With the range of frequencies measured in our devices, assuming there is no built-in strain, corresponds to a bending stiffness of 0.76–1.09 eV, which is consistent with previous theoretical and experimental work [1, 10–13].

The bending rigidity of an atomically thin sheet like graphene poses interesting questions regarding the nature of such forces [10–12, 14]. In a continuum model, the bending rigidity is related to the elastic modulus and Poisson ratio of the material; for 2D materials, this relationship makes little sense. Indeed, if one extrapolates κ from measurements of bulk graphite using the Kirchoff–Love theory of elastic plates, where a cubic dependence on the thickness is expected, one predicts a value one order of magnitude greater than that measured here and elsewhere [12]. Moreover, graphene's intrinsic ripples are also thought to play a role in its inherent stiffness [7, 15]. Further investigations including the dependence of κ on the resonator's temperature and geometry are currently underway and may reveal further surprises for this remarkable and unique material.

Acknowledgements This work was supported in part by the Director, Office of Energy Research, Office of Basic Energy Sciences, Materials Sciences and Engineering Division, of the U.S. Department of Energy under Contract #DE-AC02-05CH11231 which provided for optical vibration measurements and detailed TEM characterization; the Office of Naval Research under MURI award N00014-09-1-1066 which provided for sample synthesis; and the National Science Foundation through the Center of Integrated Nanomechanical Systems under grant #EEC-0832819 which provided for AFM characterization and student support. M. Rousseas would like to thank the Siemens Center for Knowledge Interchange for their funding. B. Alemán acknowledges support from the UC Berkeley Anselmo John Macchi Fellowship Fund in the Physical Sciences.

References

- [1] T. J. Booth, P. Blake, R. R. Nair, D. Jiang, E. W. Hill, U. Bangert, A. Bleloch, M. Gass, K. S. Novoselov, M. I. Katsnelson, and A. K. Geim, *Nano Lett.* **8**, 2442 (2008).
- [2] J. S. Bunch, A. M. van der Zande, S. S. Verbridge, I. W. Frank, D. M. Tanenbaum, J. M. Parpia, H. G. Craighead, and P. L. McEuen, *Science* **315**, 490 (2007).
- [3] C. Lee, X. Wei, J. W. Kysar, and J. Hone, *Science* **321**, 385 (2008).
- [4] I. W. Frank, D. M. Tanenbaum, A. M. van der Zande, and P. L. McEuen, *J. Vacuum Sci. Technol. B* **25**, 2558 (2007).
- [5] W. Regan, N. Alem, B. Alemán, B. Geng, Ç. Girit, L. Maserati, F. Wang, M. Crommie, and A. Zettl, *Appl. Phys. Lett.* **96**, 113102 (2010).
- [6] B. Alemán, W. Regan, S. Aloni, V. Altoe, N. Alem, C. Girit, B. Geng, L. Maserati, M. Crommie, F. Wang, and A. Zettl, *ACS Nano* **4**, 4762 (2010).
- [7] J. C. Meyer, A. K. Geim, M. I. Katsnelson, K. S. Novoselov, T. J. Booth, and S. Roth, *Nature* **446**, 60 (2007).
- [8] A. M. Van Der Zande, R. A. Barton, J. S. Alden, C. S. Ruiz-Vargas, W. S. Whitney, P. H. Q. Pham, J. Park, J. M. Parpia, H. G. Craighead, and P. L. McEuen, *Nano Lett.* **10**, 4869 (2010).
- [9] N. H. Fletcher and T. D. Rossing, *The Physics of Musical Instruments* (Springer-Verlag, New York, 1991).
- [10] Q. Wang, *Phys. Lett. A* **374**, 1180 (2010).
- [11] N. Lindahl, D. Midtvedt, J. Svensson, O. A. Nerushhev, N. Lindvall, A. Isacsson, and E. E. B. Campbell, *Nano Lett.* **12**, 3526 (2012).
- [12] Y. Wei, B. Wang, J. Wu, R. Yang, and M. L. Dunn, *Nano Lett.* **13**, 26 (2013).
- [13] Q. Lu, M. Arroyo, and R. Huang, *J. Phys. D* **42**, 102002 (2009).
- [14] P. Liu and Y. W. Zhang, *Appl. Phys. Lett.* **94**, 231912 (2009).
- [15] A. Fasolino, J. H. Los, and M. I. Katsnelson, *Nature Mater.* **6**, 858 (2007).

Editor's Note

Please, add some subheadings for the different sections of your paper, as e.g. Introduction, Experimental, Conclusion etc. Please check the quality of Figure 3.

1
2
3
4
5
6
7
8
9
10
11
12
13
14
15
16
17
18
19
20
21
22
23
24
25
26
27
28
29
30
31
32
33
34
35
36
37
38
39
40
41
42
43
44
45
46
47
48
49
50
51
52
53
54
55
56
57

WILEY-VCH
Galley Proofs